Preclinical pharmacokinetics and metabolism of a novel diaryl pyrazole resorcinol series of heat shock protein 90 inhibitors

Nicola F. Smith,[1] Angela Hayes,[1] Karen James,[1] Bernard P. Nutley,[1] Edward McDonald,[1] Alan Henley,[1] Brian Dymock,[2] Martin J. Drysdale,[2] Florence I. Raynaud,[1] and Paul Workman[1]

[1]Cancer Research UK Centre for Cancer Therapeutics at the Institute of Cancer Research, Sutton, Surrey, United Kingdom and [2]Vernalis (Cambridge) Ltd., Abington, Cambridge, United Kingdom

Abstract

CCT018159 was recently identified as a novel inhibitor of heat shock protein (Hsp) 90, a promising target for cancer therapy. Pharmacokinetic and metabolic properties are likely to be important for efficacy and need to be optimized during drug development. Here, we define the preclinical metabolism and pharmacokinetics of CCT018159 and some early derivatives. In addition, we assess *in vitro* metabolic stability screening and *in vivo* cassette dosing (simultaneous administration of several compounds to a single animal) as approaches to investigate these compounds. The plasma clearance following individual i.v. administration to mice was rapid (0.128–0.816 L/h), exceeding hepatic blood flow. For CCT066950 and CCT066952, this could be attributed in part to extensive (>80%) blood cell binding. Oral bioavailability ranged from 1.8% to 29.6%. Tissue distribution of CCT066952 was rapid and moderate, and renal excretion of the compounds was minimal (<1% of dose excreted). Compounds underwent rapid glucuronidation both *in vivo* and following incubation with mouse liver microsomes. However, whereas CCT066965 was metabolized to the greatest extent *in vitro*, this compound displayed the slowest plasma clearance. The rank order of the compounds from the highest to lowest area under the curve was the same following discrete and cassette dosing. Furthermore, pharmacokinetic variables were similar whether the compounds were dosed alone or in combination. We conclude that the pharmacokinetics of CCT018159 are complex. Cassette dosing is currently the best option available to assess the pharmacokinetics of this promising series of compounds in relatively high throughput and is now being applied to identify compounds with optimal pharmacokinetic properties during structural analogue synthesis. [Mol Cancer Ther 2006;5(6):1628–37]

Introduction

The molecular chaperone heat shock protein (Hsp) 90 is an exciting new target for cancer therapy (1–3). Hsp90 ensures the correct conformation, stability, localization, and function of ''client'' proteins, including several key oncogenic proteins such as ErbB2, Raf-1, Akt/protein kinase B, cyclin-dependent kinase 4, and mutant p53. Without functional Hsp90, these proteins undergo proteasome-mediated degradation, leading to cell cycle arrest and apoptosis (4). There is currently much interest in developing inhibitors of Hsp90 because these could potentially inhibit all of the hallmark traits of cancer (5) by depleting multiple oncogenic proteins and blocking several signal transduction pathways (1, 6, 7).

To date, most attention has focused on analogues of the benzoquinone ansamycin antibiotic geldanamycin (8), the macrocyclic antibiotic radicicol (9), and, more recently, a series of purine-scaffold small molecules derived from the rationally designed compound PU3 (10, 11). The geldanamycin derivative 17-allylamino-17-demethoxygeldanamycin is the first inhibitor of Hsp90 to enter clinical trials. Based on evidence of promising biological and clinical activity (8, 12), phase II studies of this agent are under way. However, like other known Hsp90 inhibitors, 17-allylamino-17-demethoxygeldanamycin has several limitations, such as poor solubility, low oral bioavailability (13), and metabolism by polymorphic enzymes (14, 15). Approaches to discover Hsp90 inhibitors with improved pharmacologic properties include the synthesis of structural analogues of existing inhibitors (16, 17) and the search for novel chemotypes (1, 18).

We recently developed a high-throughput screening assay for inhibitors of Hsp90 ATPase activity (19) and used this to identify the diaryl pyrazole inhibitor CCT018159 (Fig. 1) by screening a library of 60,000 compounds (20). CCT018159 inhibited Hsp90 and tumor cell growth with similar potency to 17-allylamino-17-demethoxygeldanamycin. Furthermore, consistent with Hsp90 inhibition, CCT018159 caused induction of Hsp70 and depletion of client proteins. Following identification of CCT018159 as a hit compound, the evaluation of the potential of this series of compounds to progress from hit to

Received 1/24/06; revised 3/21/06; accepted 4/13/06.

Grant support: Cancer Research UK program grant C309/A2187 and Vernalis Ltd. N.F. Smith was a recipient of a Cancer Research UK Ph.D. studentship and P. Workman is a Cancer Research UK Life Fellow.

The costs of publication of this article were defrayed in part by the payment of page charges. This article must therefore be hereby marked advertisement in accordance with 18 U.S.C. Section 1734 solely to indicate this fact.

Requests for reprints: Florence I. Raynaud, Cancer Research UK Centre for Cancer Therapeutics, Haddow Laboratories, Institute of Cancer Research, 15 Cotswold Road, Sutton, Surrey SM2 5NG, United Kingdom. Phone: 44-208-722-4212. E-mail: Florence.Raynaud@icr.ac.uk

doi:10.1158/1535-7163.MCT-06-0041

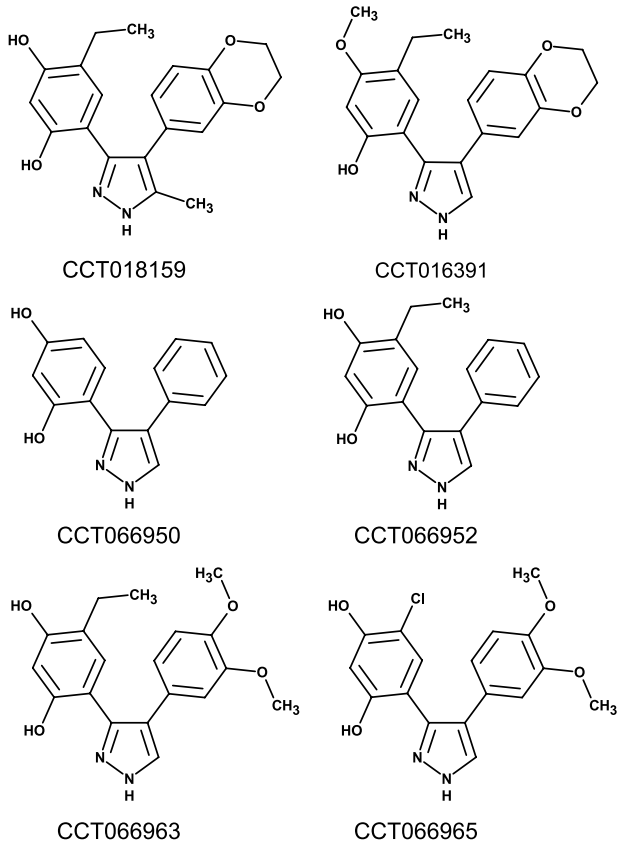

Figure 1. Chemical structures of CCT018159 analogues.

lead optimization was initiated. In addition to activity and selectivity, it was recognized that understanding the metabolism and pharmacokinetic properties of structural analogues would be important because the *in vitro* effects of CCT018159 were dependent on concentration and exposure time. Thus, activity in animal models and patients will likely require sustained compound exposures.

Evaluation of animal pharmacokinetics by conventional single compound dosing is resource-intensive and low in throughput. Indeed, pharmacokinetic analysis has become a serious bottleneck in drug discovery and a variety of higher-throughput methods have been developed in an attempt to overcome this (21). *In vitro* approaches allow for the investigation of drug absorption, metabolism, and transport in isolation, but *in vivo* studies are required to understand the combined effect of these processes on a given compound. Approaches to accelerate *in vivo* pharmacokinetic screening include sample pooling (22), the cassette-accelerated rapid rat screen (23), and cassette dosing, which involves the simultaneous administration of several compounds to a single animal (24, 25). Whereas cassette dosing reduces the number of animals used, in addition to increasing throughput, there are disadvantages of this approach, including the potential for drug-drug interactions (26, 27). The results of two recent surveys of the pharmaceutical industry suggest that cassette dosing is still widely used despite controversy surrounding this technique (28, 29). In our experience, we have found the suitability of cassette dosing to evaluate the pharmacokinetics of novel anticancer agents to be entirely dependent on the compound series under investigation. Whereas cassette dosing was recently shown to be unsuitable for a series of geldanamycin analogues due to nonlinear pharmacokinetics and drug-drug interactions (17), this approach was extremely valuable in the pharmacokinetic assessment of a large number of trisubstituted purine cyclin-dependent kinase-2 inhibitors (30).

The main objective of the current work was to gain an understanding of the preclinical pharmacokinetics and metabolism of CCT018159 and some early derivatives (Fig. 1). In addition, we wanted to assess the suitability of *in vitro* metabolic stability screening in mouse liver microsomes and *in vivo* cassette dosing in mice as methods to evaluate the pharmacokinetics of this novel diaryl pyrazole series of Hsp90 inhibitors in higher throughput during lead optimization. There are very few examples of this type of analysis in the cancer drug development literature. Because optimization of pharmacokinetic properties is frequently a rate-limiting step in the preclinical development of cancer drugs, publication of our experience may be useful in other drug discovery projects.

Materials and Methods

Chemicals and Reagents

CCT018159 and analogues were synthesized at the Cancer Research UK Centre for Cancer Therapeutics (Sutton, United Kingdom) as described (20). DMSO was obtained from Fisher Scientific UK Ltd. (Loughborough, United Kingdom). High-performance liquid chromatography grade acetonitrile and methanol were purchased from Laserchrom Analytical Ltd. (Rochester, United Kingdom). Hepatocyte thawing medium was from In Vitro Technologies (Baltimore, MD). All other chemicals and reagents were obtained from Sigma-Aldrich Company Ltd. (Gillingham, United Kingdom).

Animals and Procedures

Female BALB/c mice (6 weeks old) from Charles River UK Ltd. (Margate, United Kingdom) were kept in a controlled environment with food and sterilized water available *ad libitum*. Animals weighed 20 ± 2 g at the time of experiment. All procedures were done in accordance with the local and national guidelines for animal experimentation (31). Dosing solutions were prepared by dissolving the compounds in 10% DMSO and 5% Tween 20 in 0.9% saline. The compounds were administered i.v. and p.o., individually at 20 mg/kg and in combination at 4 mg/kg each. Animals were warmed before receiving a single i.v. bolus injection into a lateral tail vein. P.o. administration was by gavage. For urinary excretion studies, mice received 1 mL of saline i.p. immediately and ~20 hours after compound administration. Control animals received the vehicle alone. Groups of three mice were injected per time point. Blood was collected at selected time

points by cardiac puncture under anesthesia into heparinized syringes, transferred to microcentrifuge tubes, and centrifuged at 15,000 × *g* for 2 minutes to obtain plasma. For CCT066950, liver, kidney, and spleen were rapidly dissected, weighed, and snap frozen in liquid nitrogen. Urine was collected over 24 hours using Metabowl glass metabolism cages (Jencons Scientific Ltd., Leighton Buzzard, United Kingdom). Samples were stored at −20°C until analysis.

Sample Preparation

Tissues were thawed on ice and homogenized in 3 mL of PBS per gram of tissue using a PowerGen 125 Homogenizer (Fisher Scientific UK). A standard curve ranging from 50 to 50,000 nmol/L and quality control standards at 400, 4,000, and 40,000 nmol/L were prepared in 100 μL of blank plasma or tissue homogenate. CCT016391 was added to all standards and samples as an internal standard. Proteins were precipitated by the addition of 3 volumes of methanol. Samples were centrifuged at 2,800 × *g* for 10 minutes at 4°C and the supernatants were removed for analysis. Urine volumes were measured before diluting an aliquot 1:10 with methanol. Standards were prepared at 10, 100, 1,000, and 10,000 nmol/L in diluted blank urine. CCT016391 was added as an internal standard and samples were centrifuged at 2,000 × *g* for 10 minutes at room temperature.

β-Glucuronidase Hydrolysis

One hundred-sixty units of β-glucuronidase (type B-1 from bovine liver), dissolved in ammonium acetate (pH 5), were added in duplicate to 20-μL aliquots of plasma pooled from three mice treated with 20 mg/kg CCT066963. Incubations were done at 37°C for 1 hour. Control incubations were done in the absence of β-glucuronidase. The reaction was terminated by the addition of 3 volumes of methanol and plasma samples were processed as described above.

Blood Cell Binding

Fresh blood was obtained from untreated animals and plasma was prepared by centrifugation. Aliquots of plasma and blood were added to test compound in duplicate to give a final concentration of 10 μmol/L. Incubations were carried out for 20 minutes at 37°C. Spiked blood samples were centrifuged to obtain plasma. To equal volumes (100 μL) of spiked plasma or plasma obtained from spiked blood, CCT016391 was added as an internal standard and samples were processed as described above.

Microsomal Incubations

Male CD1 mouse liver microsomes and male pooled human liver microsomes were purchased from XenoTech LLC (Lenexa, KS) and pooled human intestinal microsomes were from In Vitro Technologies. Incubations contained final concentrations of 1 mg/mL microsomal protein, 10 μmol/L test compound, 3 mmol/L $MgCl_2$, 1 mmol/L NADPH, 2.5 mmol/L UDP-glucuronic acid, and 50 mmol/L phosphate buffer (pH 7.4) in a total volume of 200 μL and were done for 5 minutes at 37°C. The reaction was terminated by the addition of 2 volumes of ice-cold methanol and CCT016391 was added as an internal standard. $T_{0\ min}$ samples were prepared in exactly the same way except that the test compound was added immediately after the addition of methanol. Samples were centrifuged at 2,800 × *g* for 10 minutes at 4°C and the supernatants analyzed. 7-Hydroxycoumarin (the positive control used for the hepatocyte experiments) was incubated at a final concentration of 100 μmol/L with human liver microsomes supplemented with UDP-glucuronic acid only for 30 minutes to generate 7-hydroxycoumarin glucuronide.

Hepatocyte Incubations

Human hepatocytes (from two male donors) were purchased from In Vitro Technologies (Leipzig, Germany). Krebs-Henseleit buffer was supplemented with 1 mmol/L calcium chloride, 28.5 mmol/L sodium bicarbonate, 84 μg/mL amikacin sulfate, 84 μg/mL gentamicin, 20 mmol/L HEPES, and 4.2 μmol/L heptanoic acid and the pH was adjusted to 7.4. After thawing, heptatocytes were resuspended in 48 mL of prewarmed hepatocyte thawing media and centrifuged at 50 × *g* for 5 minutes. This was followed by removal of the supernatant and resuspension in Krebs-Henseleit buffer. The viability (86.9%) and cell density were measured by trypan blue exclusion. The test compounds and 7-ethoxycoumarin were incubated at 10 and 100 μmol/L, respectively, with 1 million hepatocytes/mL. The final methanol and DMSO concentrations were 0.5% and 0.1%, respectively. Incubations were done in 20-mL glass scintillation vials in a static, 37°C, 5% CO_2 incubator. Aliquots were removed at selected time points and quenched with 3 volumes of methanol (test compounds) or 25% of the incubation volume of 70% perchloric acid (7-ethoxycoumarin). CCT016391 was added as an internal standard. Samples were centrifuged at 15,000 × *g* for 10 minutes at room temperature and the supernatants removed for analysis. Incubations of CCT018159 and CCT066965 were done in duplicate.

Sample Analysis

Chromatography was done using a Supelcosil Discovery C18 column (5 cm × 4.6 mm ID, 5 μm; Supelco, Gillingham, United Kingdom). The mobile phase consisted of methanol and 0.1% formic acid in water. Methanol was increased from 10% to 90% over 6.5 minutes, held at 90% for 5.5 minutes, returned to 10% over 0.5 minutes, and held for 5 minutes. The flow rate was 0.6 mL/min and the sample injection volume was 20 μL. A TSQ 700 triple quadrupole instrument (ThermoFinnigan, Hemel Hempstead, United Kingdom) coupled to a 600 MS pump and 717 autosampler (Waters Ltd., Elstree, United Kingdom) was used for quantitative analysis. The mass spectrometer was equipped with an electrospray source and operated in positive mode. The capillary temperature and spray voltage were operated at 260°C and 5.5 kV, respectively. The sheath, auxiliary, and collision gas flows were set at 60, 15, and 1.2 arbitrary units, respectively. Detection was done by multiple reaction monitoring of the following transitions: CCT018159, *m/z* 352 → *m/z* 283; CCT016391, *m/z* 352 → *m/z* 324; CCT066950, *m/z* 253 → *m/z* 183; CCT066952, *m/z* 281 → *m/z* 253; CCT066963, *m/z* 341 → *m/z* 325; and

CCT066965, *m/z* 347 → *m/z* 331. The limit of quantitation ranged from 50 to 250 nmol/L, depending on the compound, and standard curves were linear up to 50,000 nmol/L. Quality control standards were within 15% of nominal concentrations.

For 7-ethoxycoumarin hepatocyte incubations, chromatography was done using a Hypersil BDS C8 column (25 cm × 4.6 mm ID, 5 μm; Supelco). The mobile phase consisted of 0.1% trifluoroacetic acid in acetonitrile and 0.1% trifluoroacetic acid in water. Acetonitrile was increased from 0% to 10% over 10 minutes, from 10% to 40% over 5 minutes, from 40% to 60% over 10 minutes, returned to 0% over 1 minute, and held for 5 minutes. The flow rate was 1 mL/min and the sample injection volume was 20 μL. Detection was by UV absorbance at 320 nm using a UV6000 detector connected to a SpectraSYSTEM AS3000 autosampler and P4000 pump (ThermoFinnigan).

An LCQ ion trap instrument coupled to a SpectraSYSTEM P4000 pump and an AS3000 autosampler (ThermoFinnigan) was used for qualitative analysis. The mass spectrometer was equipped with an electrospray source and operated in positive mode. The capillary temperature and spray voltage were operated at 250°C and 4.5 kV, respectively. Sheath and auxiliary gases were set to 80 and 20 arbitrary units, respectively. Spectra were acquired in full-scan mode over the *m/z* range 150 to 850. The sample injection volume was 25 μL.

Sample Processing

Pharmacokinetics. Ratios of the peak area of each analyte to that of the internal standard were calculated. Plasma and tissue concentrations were interpolated from standard curves constructed by linear regression using GraphPad Prism Version 3.02 (GraphPad Software, Inc., San Diego, CA). Mean concentrations ($n = 3$) for each time point were calculated. Urine concentrations were converted to nanomoles excreted based on the volume of urine collected and the percent of the dose excreted was calculated. Pharmacokinetic variables were evaluated by noncompartmental analysis using WinNonlin Professional Version 3.2 (Pharsight Corporation, Mountain View, CA).

Metabolism. Metabolic stability was assessed by monitoring disappearance of the parent compound over the incubation period. Full-scan spectra were manually inspected for peaks that were present following incubation with microsomes and hepatocytes, and in plasma and tissue samples from treated animals but absent in control samples. Possible metabolites were determined by the mass difference from the parent compound. Ratios of the peak area of each possible metabolite and the parent compound to the internal standard were calculated.

Statistical Analysis. A previously described method (32) was used to estimate the variance of area under the curve (AUC) calculated to the last observation (AUC_{last}) based on the variance of the mean concentration ($n = 3$) at each time point. A Z test was used for pairwise comparison of AUCs and observed $Z > 1.96$ indicated a significant difference (33). All other statistical analyses were done using GraphPad Prism Version 3.02 (GraphPad Software).

Results

Pharmacokinetics following Discrete Dosing

The plasma concentration-time curves of the compounds following individual i.v. and p.o. administration are shown in Fig. 2A and B, respectively. Oral absorption of the compounds was rapid, with peak plasma levels observed 5 minutes after administration (Fig. 2B). CCT018159 displayed equally fast absorption from the peritoneal cavity (data not shown). CCT066965 exhibited the highest maximum concentration and AUC following administration by both routes (Table 1). The plasma clearance of the compounds was rapid, ranging from 0.128 L/h for CCT066965 to 0.816 L/h for CCT066952. Plasma clearance and half-life of CCT018159 were similar regardless of the route of administration. The oral bioavailability of the compounds was relatively low, ranging from 1.8% for CCT018159 to 29.6% for CCT066965. Phenyl substitutions at position 4 of the pyrazole seem to play a role in the pharmacokinetics of this compound series. The two compounds that reached the highest plasma levels (i.e., CCT066965 and CCT066963) have two methoxy substituents on this ring whereas CCT066952 and CCT066950 do not. Substitutions at position 5 of the resorcinol ring do not seem to be important in terms of exposure.

Distribution of CCT066950 to the liver, kidneys, and spleen was rapid following i.v. and p.o. dosing, with maximum tissue levels observed at 5 minutes (data not shown). CCT066950 levels were highest in the kidneys, followed by the spleen, plasma, and liver (Table 1). Tissue-to-plasma AUC ratios were similar following i.v. and p.o. administration. Clearance from the kidneys and the spleen was similar, the values being 0.147 and 0.190 L/h, respectively. Plasma and liver clearances were 3.9-fold and 8.7-fold faster, respectively.

The urinary excretion of all five compounds was minimal, with <1% of the dose being excreted as unchanged parent over 24 hours.

In vivo Metabolism

Initially, metabolites were tentatively identified by mass difference from the parent compound. The major route of metabolism seemed to be glucuronide conjugation, with both monoglucuronide and bisglucuronide conjugates observed. Some of the compounds also underwent oxidative metabolism, including hydroxylation and demethylation. Assuming that the mass spectral responses of the parent compounds and the proposed metabolites were the same, the ratio of the proposed glucuronide conjugates to the parent at the first sampling time of 5 minutes was calculated. This gave values ranging from 1.94 for CCT066965, which displayed a relatively slow plasma clearance, to 16.87 for CCT066950, which was rapidly cleared from plasma. The tentative identification of glucuronide conjugates was confirmed by incubation of plasma obtained from CCT066963-treated mice with β-glucuronidase. This led to an increase in levels of the parent compound, confirmed with an authentic standard, and a corresponding decrease in the glucuronide conjugates (data not shown).

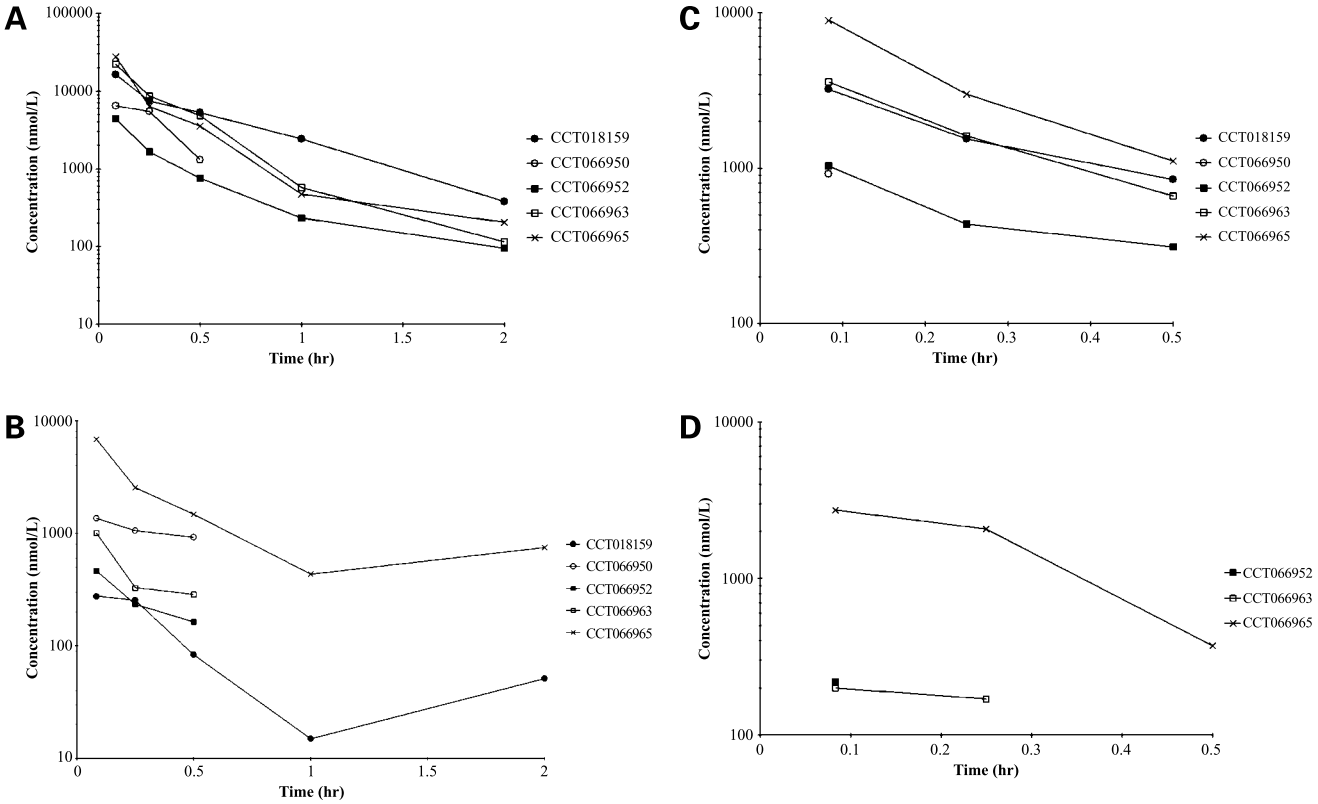

Figure 2. Plasma concentration-time curves of CCT018159 analogues following individual (**A**, i.v.; **B**, p.o.) and cassette (**C**, i.v.; **D**, p.o.) administration to mice. CCT018159, CCT066950, CCT066952, CCT066963, and CCT066965 were administered in combination at 4 mg/kg each and individually at 20 mg/kg.

In vitro Metabolism

Preliminary assay optimization experiments revealed that the compounds were extensively metabolized by mouse liver microsomes over a period of 30 minutes. Thus, an incubation time of 5 minutes was selected for further studies. Mouse liver microsomal incubations (n = 3) were reproducible, with coefficients of variation ranging from 0.41% for CCT066965, which was metabolized to the greatest extent, to 10.2% for CCT018159, which was the least metabolized compound. Microsomal metabolism was rapid and extensive, with near complete loss of parent observed for some of the compounds (Table 2). The extent of parent loss was similar whether the microsomes were supplemented with both NADPH and UDP-glucuronic acid or with UDP-glucuronic acid alone (data not shown). With the exception of CCT018159, compounds were metabolized to a greater extent by mouse compared with human liver microsomes (Table 2). However, the lower cytochrome *P*450 (and possibly UDP-glucuronosyltransferase) content of the human microsomal preparation has to be taken into account. Despite differences in the extent of parent loss, ranking from the least to the most metabolized compound was the same between the two species, with the exception of CCT018159. The extent of human intestinal metabolism was less than that of hepatic metabolism. This was most pronounced for CCT066950, which did not undergo intestinal metabolism, yet parent loss following incubation with liver microsomes was 43.7%.

In vitro metabolic stability in microsomes was not predictive of *in vivo* plasma clearance with regards to compound ranking, with a major discrepancy observed for CCT066965 in particular. Of the compounds studied, CCT066965 was metabolized to the greatest extent *in vitro* (98.2% parent loss) but displayed the slowest plasma clearance *in vivo* (Table 1).

The proposed metabolites formed by mouse liver microsomes *in vitro* were similar to those formed by the mouse following *in vivo* administration. In addition, the same metabolites were observed following compound incubation with both the mouse and human microsomal preparations. None of the compounds underwent oxidative metabolism when incubated with the human liver microsomes, with only proposed glucuronide conjugates observed.

Four of the five compounds were completely metabolized by human hepatocytes within 60 minutes (data not shown). Loss of the positive control 7-ethoxycoumarin was 18.5% and the metabolites 7-hydroxycoumarin and its glucuronide and sulfate conjugates were identified. Hepatocyte metabolism compared well with that by human liver

Table 1. Pharmacokinetic variables of CCT018159 analogues following individual administration to mice at 20 mg/kg

Compound	Tissue	Route	AUC_{last} (h*nmol/L)	AUC_{INF} (h*nmol/L)	C_{max} (nmol/L)	CL/F, obs (L/h)	HL (h)	V_z/F, obs (Liter)	F	Tissue/ plasma AUC
CCT018159	Plasma	i.v.	8,610	8,823	24,208	0.129	0.39	0.073	—	—
CCT018159	Plasma	p.o.	155	206	275	5.50	0.69	5.471	0.018	—
CCT066950	Plasma	i.v.	2,408	2,738	7,088	0.580	0.17	0.146	—	—
CCT066950	Plasma	p.o.	505	1,548	1,355	1.025	0.78	1.157	0.210	—
CCT066950	Liver	i.v.	1,081	1,243	4,430	1.277	0.17	0.321	—	0.4
CCT066950	Liver	p.o.	319	ND*	1,957	ND*	ND*	ND*	—	0.6
CCT066950	Kidney	i.v.	10,551	10,821	66,607	0.147	0.09	0.020	—	4.4
CCT066950	Kidney	p.o.	2,188	2,641	10,604	0.601	0.17	0.149	—	4.3
CCT066950	Spleen	i.v.	7,151	8,338	23,582	0.190	0.19	0.051	—	3.0
CCT066950	Spleen	p.o.	1,304	1,708	5,048	0.930	0.22	0.290	—	2.6
CCT066952	Plasma	i.v.	1,690	1,750	7,098	0.816	0.44	0.520	—	—
CCT066952	Plasma	p.o.	127	195	463	7.337	0.29	3.036	0.075	—
CCT066963	Plasma	i.v.	8,358	8,400	35,833	0.140	0.26	0.052	—	—
CCT066963	Plasma	p.o.	229	331	1,002	3.554	0.25	1.264	0.027	—
CCT066965	Plasma	i.v.	8,912	9,014	57,235	0.128	0.35	0.065	—	—
CCT066965	Plasma	p.o.	2,641	3,363	6,863	0.343	0.67	0.332	0.296	—

Abbreviations: AUC_{last}, AUC up to the time of the last measurable concentration; AUC_{INF}, AUC from the time of dosing extrapolated to infinity; C_{max}, maximum concentration; CL, total body clearance; HL terminal half-life; V_z, volume of distribution based on the terminal phase.
*Not determined (not enough time points with compounds detected).

microsomes. The extent of metabolism during a 30-minute hepatocyte incubation was comparable to that during a 5-minute microsomal incubation. In addition, the rank order from the least to the most extensively metabolized compound was the same in both preparations, with the exception of CCT018159 (CCT066963 > CCT066950 > CCT066952 > CCT066965 > CCT018159 for the hepatocytes). There was no evidence of sulfate conjugation following incubation of the test compounds with hepatocytes.

Cassette Dosing

The plasma concentration-time curves of the compounds following i.v. and p.o. administration in combination at 4 mg/kg each are shown in Fig. 2C and D, respectively. CCT018159 and CCT066950 were undetectable following cassette administration by the p.o. route. Following i.v. administration, the compounds displayed approximately linear increases in AUC and maximum plasma concentration as the dose was increased 5-fold from 4 mg/kg for cassette dosing to 20 mg/kg for discrete dosing (when calculated up to the time of the last measurable concentration in the cassette; Table 3). Furthermore, the dose-normalized AUC, plasma clearance, half-life, and volume of distribution were similar whether the compounds were dosed alone or in combination (Table 3). Of the four compounds, the cassette versus discrete dosing pharmacokinetic variables differed most for CCT066965. Plasma clearance of this compound following cassette dosing was 60% of that following single compound dosing, the values being 0.084 and 0.139 L/h, respectively. However, the half-life was similar whether it was dosed alone or in combination. The rank order of the compounds from the highest to the lowest AUC following cassette dosing was similar to that following discrete dosing, whether the AUCs were calculated up to the same time point or using all measurable concentrations (Table 4). Statistical analysis revealed that the AUC of CCT066965, which had the highest AUC following single compound administration, was not significantly different from that of CCT018159 or CCT066963, which ranked second and third, respectively. In addition, the AUCs of CCT066950 and CCT066952, which ranked fourth and fifth, were not significantly different ($Z_{obs} < 1.96$). Following cassette administration, the AUC of CCT066965 was significantly higher than that of the other compounds. However, there was no significant difference between the AUCs of the compounds that ranked second and third (i.e., CCT066963 and CCT018159, respectively). With the exception of CCT066965 ($Z_{obs} = 2.96$), there were no significant differences between the dose-normalized AUCs of the analogues following cassette

Table 2. Parent loss of CCT018159 analogues following a 5-minute incubation at 10 μmol/L with mouse liver microsomes, human liver microsomes, and human intestinal microsomes

Compound	% Parent loss		
	Mouse liver microsomes	Human liver microsomes	Human intestinal microsomes
CCT018159	58.0 (3.40)	85.5	65.3
CCT066950	73.7 (2.48)	43.7	0
CCT066952	88.9 (2.43)	74.8	26.4
CCT066963	70.5 (1.33)	43.2	33.6
CCT066965	98.2 (0.23)	96.7	89.9

NOTE: Mouse liver microsome incubations were done in triplicate. The SE is shown in parenthesis.

Table 3. Comparison of the plasma pharmacokinetic variables of CCT018159 analogues following cassette and single compound administration

Compound	Administration	Route	T_{last} (h)	AUC_{last} (h nmol/L)	AUC_{INF} (h nmol/L)	C_{max} (nmol/L)	CL/F, obs (L/h)	HL (h)	V_z/F, obs (Liter)
CCT018159	Cassette	i.v.	0.5	1,023 (110)	1,294.4	4,632.3	0.176	0.221	0.056
CCT018159	Individual	i.v.	0.5	5,279 (492)	7,282.9	24,207.8	0.156	0.264	0.059
CCT018159	Individual	i.v.	2	8,610 (1,068)	8,823.3	24,207.8	0.129	0.391	0.073
CCT066952	Cassette	i.v.	0.5	326 (44.5)	439.1	1,591.3	0.651	0.252	0.236
CCT066952	Individual	i.v.	0.5	1,280 (96.2)	1,461.8	7,098.0	0.977	0.168	0.236
CCT066952	Individual	i.v.	2	1,690 (113)	1,750.1	7,098.0	0.816	0.442	0.520
CCT066963	Cassette	i.v.	0.5	1,086 (160)	1,250.8	5,300.4	0.188	0.173	0.047
CCT066963	Individual	i.v.	0.5	6,659 (156)	8,020.0	35,832.9	0.147	0.195	0.041
CCT066963	Individual	i.v.	2	8,358 (317)	8,400.1	35,832.9	0.140	0.255	0.052
CCT066965	Cassette	i.v.	0.5	2,519 (327)	2,743.7	15,370.6	0.084	0.141	0.017
CCT066965	Individual	i.v.	0.5	7,569 (429)	8,324.2	57,235.1	0.139	0.147	0.029
CCT066965	Individual	i.v.	2	8,912 (526)	9,014.0	57,235.1	0.128	0.350	0.065
CCT066963	Cassette	p.o.	0.25	39.1	ND*	199.2	ND*	ND*	ND*
CCT066963	Individual	p.o.	0.25	153	ND*	1,001.5	ND*	ND*	ND*
CCT066963	Individual	p.o.	0.5	229	331.0	1,001.5	3.554	0.246	1.264
CCT066965	Cassette	p.o.	0.5	817	892.0	2,722.0	0.259	0.140	0.052
CCT066965	Individual	p.o.	0.5	1,574	1,985.8	6,862.7	0.116	0.194	0.033
CCT066965	Individual	p.o.	2	2,641	3,363	6,862.7	0.343	0.670	0.332

NOTE: Compounds were administered individually at 20 mg/kg and in combination at 4 mg/kg each. The SD of the AUC_{last} is given in parentheses. T_{last}, time of last measurable positive concentration.
*Not calculable due to limited number of detectable time points.

and single compound administration. When CCT066965 was administered p.o., the increases in AUC and the maximum concentration with the 5-fold increase in dose between cassette and single compound dosing were less than proportional (~2-fold). The plasma clearance and the volume of distribution were 2.2- and 1.6-fold higher, respectively, following cassette compared with discrete dosing and the half-life was 38.6% longer after single compound administration.

Red Blood Cell Binding

Of the five compounds, CCT066950 and CCT066952 bound to the cellular constituents of blood. Figure 3 shows that blood cell binding was highly correlated with plasma clearance (R^2 = 0.90), AUC (R^2 = 0.98), and molecular weight (R^2 = 0.97).

Discussion

This work describes the preclinical pharmacokinetics and metabolism of a promising and novel series of Hsp90 inhibitors (18, 20). The diaryl pyrazole compounds exhibited rapid plasma clearance and relatively low oral bioavailability (1.8–29.6%; Table 1). Distribution of CCT066950 to the liver, kidneys, and spleen was rapid but variable, resulting in tissue-to-plasma AUC ratios of 0.4, 4.4, and 3.0, respectively (Table 1). Because renal excretion was minimal, metabolism was thought to play a major role in the elimination of these compounds.

The preliminary identification of glucuronidation as the major route of metabolism was later confirmed by incubation of plasma with β-glucuronidase (data not shown), which revealed that conjugation occurs at the

Table 4. Ranking of CCT018159 analogues from the highest (top) to the lowest (bottom) AUC following cassette and single compound i.v. administration

Cassette		Individual*		Individual†	
AUC_{last}	AUC_{INF}	AUC_{last}	AUC_{INF}	AUC_{last}	AUC_{INF}
CCT066965	CCT066965	CCT066965	CCT066965	CCT066965	CCT066965
CCT066963	CCT018159	CCT066963	CCT066963	CCT018159	CCT018159
CCT018159	CCT066963	CCT018159	CCT018159	CCT066963	CCT066963
CCT066952	CCT066952	CCT066950	CCT066950	CCT066950	CCT066950
CCT066950‡	CCT066950‡	CCT066952	CCT066952	CCT066952	CCT066952

*Calculated up to the time of the last measurable concentration following cassette dosing.
†Calculated up to the time of the last measurable concentration following single compound dosing.
‡CCT066950 was only detectable for up to 5 minutes following cassette dosing.

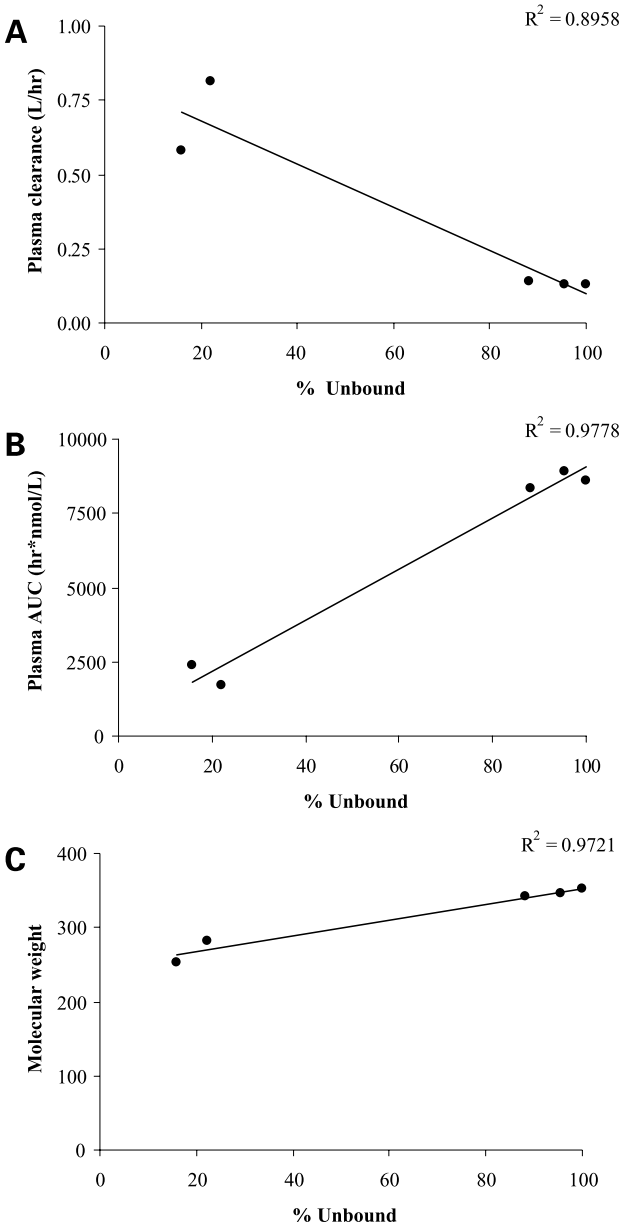

Figure 3. Relationship between blood cell binding and plasma clearance (**A**), AUC (**B**), and molecular weight (**C**) of the CCT018159 analogues.

hydroxyl groups on the resorcinol ring. The liver represents one of the major sites of glucuronidation; however, UDP-glucuronosyltransferases are also expressed in extrahepatic tissues (34). Kidney levels of CCT066950 were 10-fold higher than those in the liver, and clearance from the kidney and spleen was similar (Table 1). These factors suggest that glucuronidation occurs predominantly in the liver. However, because glucuronide conjugates were formed by human intestinal microsomes, it is likely that glucuronidation occurs in the mouse intestine, thus contributing to the low oral bioavailability observed. Species differences in the elimination pathways of the resorcinol terbutaline have been described (35), with glucuronidation being predominant over sulfation in the rat but not in man. In the current study, there was no evidence of sulfation in the mouse *in vivo* or following compound incubation with human hepatocytes.

Because *in vivo* studies revealed that the compounds underwent extensive metabolism, we proposed that a metabolism-based screen would be potentially useful to rank further analogues during lead optimization and limit the number required for *in vivo* evaluation. Although glucuronide conjugation was the major metabolic route, some of the compounds also underwent oxidative metabolism; thus, microsomes were supplemented with both NADPH and UDP-glucuronic acid. The microsomal incubations were useful in that the identities of the metabolites produced were the same as those produced *in vivo*. In addition, compounds underwent rapid and extensive turnover *in vitro* as they did *in vivo.* However, *in vitro* metabolic stability was not predictive of plasma clearance with regards to compound ranking. This was most evident for CCT066965, which underwent 98.2% parent loss *in vitro*, yet displayed the slowest plasma clearance of the compounds following individual and cassette administration by the i.v. and p.o. routes (Tables 1 and 3). Notably, CCT066965 was also the most extensively metabolized compound by human liver and intestinal microsomes (Table 2). It is possible that the compounds undergo extrahepatic glucuronidation and distribution of CCT066965 to sites of metabolism is less extensive than that of the other compounds. To determine whether the discrepancy between the microsomal and *in vivo* data was influenced by hepatocellular uptake, the compounds were incubated with hepatocytes. Hepatocyte metabolism was slower and less extensive than microsomal metabolism but the rank order from the most to the least metabolized compound was similar. Although metabolism is clearly of importance for this compound series, the fact that the plasma clearance of the compounds investigated approximates or exceeds mouse liver blood flow (0.108 L/h; ref. 36) suggests that the elimination of these compounds may in fact be governed by liver blood flow rather than intrinsic metabolism. This may explain the observed lack of *in vitro-in vivo* correlation.

Due to the discrepancies observed between plasma clearance and metabolic stability in microsomes, the suitability of cassette dosing was assessed. Following i.v. administration, the rank order from the highest to the lowest AUC following cassette dosing was similar to that observed following individual administration (Table 4). The magnitudes of the differences between the pharmacokinetic variables following cassette and single compound dosing were similar to or less than those reported in the few published studies that provide these comparative data (37–39). The current compounds generally displayed linear pharmacokinetics between cassette dosing at 4 mg/kg and discrete dosing at 20 mg/kg (Table 3). Furthermore, the pharmacokinetic variables following single and cassette

dosing were very similar. With the exception of CCT066965, there were no significant differences between the dose-normalized AUCs of the compounds following cassette and single compound i.v. dosing.

The observed rapid clearances could be explained in part by extrahepatic metabolism and/or elimination of the compounds by another mechanism. However, as the liver is the most highly perfused organ, it is unlikely that metabolism by another organ could account for the clearances observed. Furthermore, renal excretion of these compounds was minimal. Because the resorcinol compound terbutaline has an affinity for red blood cells (40), the extent of binding of the current compounds to the cellular constituents of blood was investigated. If a compound was extensively bound, then a considerable amount would be discarded after centrifugation of blood to obtain plasma, resulting in a high blood-to-plasma ratio. Consequently, plasma concentrations would be lower than the actual blood concentrations *in vivo* at the time of sampling, resulting in a low AUC and a corresponding fast plasma clearance. Experiments were conducted at room temperature and at 37°C and similar results were obtained at both temperatures (data not shown). Two of the compounds were extensively bound and the extent of binding was highly correlated with plasma clearance (R^2 = 0.90) and AUC (R^2 = 0.98; Fig. 3), suggesting that the rapid plasma clearances observed for CCT066950 and CCT066952 are largely a consequence of their affinity for red blood cells. Blood cell binding also seemed to be dependent on molecular weight (R^2 = 0.97). Note, however, that with the data available, it is still possible that the relationship between blood cell binding is more dichotomous than continuous. Interestingly, mature human erythrocytes have been shown to express Hsp90, the target of the current compounds (41). However, there was no apparent correlation between blood cell binding and the IC_{50} values for Hsp90 inhibition (data not shown). The effect of blood cell binding on the tissue distribution and metabolism of the current compounds requires further investigation, although in the optimization of these compounds an objective would be to eliminate this property.

To conclude, the present studies have shown that the metabolism and pharmacokinetics of CCT018159 and its analogues are complex. Although *in vivo* studies suggest that the elimination of these compounds is limited by hepatic blood flow rather than intrinsic metabolism, glucuronidation does seem to be of importance. Structural modification will be required to decrease glucuronide conjugation or increase potency as one or both of the phenolic groups on the resorcinol ring seem to be required for Hsp90 inhibitory activity (20). The importance of carrying out detailed studies of a few members of a compound series before considering methods to evaluate the pharmacokinetics of a larger number of that series in higher throughput has been shown. Furthermore, the advantages of assessing several screening methods before selecting the most appropriate one for use during lead optimization have been shown. The fact that parent loss of the compounds in human hepatocytes reflects that seen in human liver microsomes suggests that the incubation conditions used to study the oxidation and glucuronidation of the current compounds in microsomes could be relevant to the human situation. However, the extent of parent loss in microsomes was not predictive of *in vivo* pharmacokinetics in mice with regards to compound ranking. In light of the current studies, the binding of further CCT018159 analogues to the cellular constituents of blood should be determined routinely. If a compound is extensively bound, then plasma may not be the most appropriate assay matrix in which to evaluate its pharmacokinetics. For compounds that are not bound to blood cells, which as mentioned is a desirable feature from the point of view of further drug development, cassette dosing is currently the best option available to assess the *in vivo* pharmacokinetics of the current series of compounds in relatively high throughput following i.v. administration, and is currently being used in lead optimization, alongside other biological assays, to select a clinical development candidate for the CCT018159 series.

There are relatively few published examples of the use of higher-throughput techniques, particularly cassette dosing (17, 30), in the preclinical development of cancer drugs. The process used and experience presented here may therefore be of interest and value to investigators seeking to optimize the properties of other classes of molecular cancer therapeutics. The use of such methods is not only more efficient than single compound evaluation but it can also result in decreased animal usage.

Acknowledgments

We thank Rob Gilbert for his assistance with the animal experiments.

References

1. Maloney A, Workman P. HSP90 as a new therapeutic target for cancer therapy: the story unfolds. Expert Opin Biol Ther 2002;2:3 – 24.

2. Workman P. Overview: translating Hsp90 biology into Hsp90 drugs. Curr Cancer Drug Targets 2003;3:297 – 300.

3. Chiosis G, Vilenchik M, Kim J, Solit D. Hsp90: the vulnerable chaperone. Drug Discov Today 2004;9:881 – 8.

4. Hostein I, Robertson D, DiStefano F, Workman P, Clarke PA. Inhibition of signal transduction by the Hsp90 inhibitor 17-allylamino-17-demethoxygeldanamycin results in cytostasis and apoptosis. Cancer Res 2001;61:4003 – 9.

5. Hanahan D, Weinberg RA. The hallmarks of cancer. Cell 2000;100:57 – 70.

6. Workman P. Altered states: selectively drugging the Hsp90 cancer chaperone. Trends Mol Med 2004;10:47 – 51.

7. Workman P. Combinatorial attack on multistep oncogenesis by inhibiting the Hsp90 molecular chaperone. Cancer Lett 2004;206:149 – 57.

8. Sausville EA, Tomaszewski JE, Ivy P. Clinical development of 17-allylamino, 17-demethoxygeldanamycin. Curr Cancer Drug Targets 2003;3:377 – 83.

9. Soga S, Shiotsu Y, Akinaga S, Sharma SV. Development of radicicol analogues. Curr Cancer Drug Targets 2003;3:359 – 69.

10. Chiosis G, Lucas B, Huezo H, et al. Development of purine-scaffold small molecule inhibitors of Hsp90. Curr Cancer Drug Targets 2003;3:371 – 6.

11. Wright L, Barril X, Dymock B, et al. Structure-activity relationships in purine-based inhibitor binding to HSP90 isoforms. Chem Biol 2004;11:775 – 85.

12. Banerji U, O'Donnell A, Scurr M, et al. Phase I pharmacokinetic and pharmacodynamic study of 17-allylamino, 17-demethoxygeldanamycin in patients with advanced malignancies. J Clin Oncol 2005;23:4152 – 61.

13. Egorin MJ, Zuhowski EG, Rosen DM, et al. Plasma pharmacokinetics and tissue distribution of 17-(allylamino)-17-demethoxygeldanamycin (NSC 330507) in CD2F1 mice1. Cancer Chemother Pharmacol 2001;47: 291 – 302.

14. Egorin MJ, Rosen DM, Wolff JH, et al. Metabolism of 17-(allylamino)-17-demethoxygeldanamycin (NSC 330507) by murine and human hepatic preparations. Cancer Res 1998;58:2385 – 96.

15. Kelland LR, Sharp SY, Rogers PM, Myers TG, Workman P. DT-Diaphorase expression and tumor cell sensitivity to 17-allylamino, 17-demethoxygeldanamycin, an inhibitor of heat shock protein 90. J Natl Cancer Inst 1999;91:1940 – 9.

16. Egorin MJ, Lagattuta TF, Hamburger DR, et al. Pharmacokinetics, tissue distribution, and metabolism of 17-(dimethylaminoethylamino)-17-demethoxygeldanamycin (NSC 707545) in CD2F1 mice and Fischer 344 rats. Cancer Chemother Pharmacol 2002;49:7 – 19.

17. Smith NF, Hayes A, Nutley BP, Raynaud FI, Workman P. Evaluation of the cassette dosing approach for assessing the pharmacokinetics of geldanamycin analogues in mice. Cancer Chemother Pharmacol 2004;54: 475 – 86.

18. Dymock B, Barril X, Brough PA, et al. Novel, potent small molecule inhibitors of the molecular chaperone Hsp90 discovered through structure-based design. J Med Chem 2005;48:4212 – 5.

19. Rowlands MG, Newbatt YM, Prodromou C, et al. High-throughput screening assay for inhibitors of heat-shock protein 90 ATPase activity. Anal Biochem 2004;327:176 – 83.

20. Cheung KM, Matthews TP, James K, et al. The identification, synthesis, protein crystal structure and *in vitro* biochemical evaluation of a new 3,4-diarylpyrazole class of Hsp90 inhibitors. Bioorg Med Chem Lett 2005;15:3338 – 43.

21. Roberts SA. Drug metabolism and pharmacokinetics in drug discovery. Curr Opin Drug Discov Devel 2003;6:66 – 80.

22. Kuo BS, Van Noord T, Feng MR, Wright DS. Sample pooling to expedite bioanalysis and pharmacokinetic research. J Pharm Biomed Anal 1998;16:837 – 46.

23. Korfmacher WA, Cox KA, Ng KJ, et al. Cassette-accelerated rapid rat screen: a systematic procedure for the dosing and liquid chromatography/atmospheric pressure ionization tandem mass spectrometric analysis of new chemical entities as part of new drug discovery. Rapid Commun Mass Spectrom 2001;15:335 – 40.

24. Frick LW, Adkinson K, Wells-Knecht K, Woollard P, Higton D. Cassette dosing: rapid in vivo assessment of pharmacokinetics. Pharm Sci Technol Today 1998;1:12 – 8.

25. Bayliss MK, Frick LW. High-throughput pharmacokinetics: cassette dosing. Curr Opin Drug Discov Devel 1999;2:20 – 5.

26. Frick LW, Higton D, Wring S, Wells-Knecht K. Cassette dosing: rapid estimation of in vivo pharmacokinetics. Med Chem Res 1998;8:472 – 7.

27. White RE, Manitpisitkul P. Pharmacokinetic theory of cassette dosing in drug discovery screening. Drug Metab Dispos 2001;29:957 – 66.

28. Ackermann BL. Results from a bench marking survey on cassette dosing practices in the pharmaceutical industry. J Am Soc Mass Spectrom 2004;15:1374 – 7.

29. Manitpisitkul P, White RE. Whatever happened to cassette-dosing pharmacokinetics? Drug Discov Today 2004;9:652 – 8.

30. Raynaud FI, Fischer PM, Nutley BP, et al. Cassette dosing pharmacokinetics of a library of 2,6,9-trisubstituted purine cyclin-dependent kinase 2 inhibitors prepared by parallel synthesis. Mol Cancer Ther 2004; 3:353 – 62.

31. Workman P, Twentyman P, Balkwill F, et al. United Kingdom Co-ordinating Committee on Cancer Research (UKCCCR) guidelines for the welfare of animals in experimental neoplasia (2nd ed.). Br J Cancer 1998; 77:1 – 10.

32. Bailer AJ. Testing for the equality of area under the curves when using destructive measurement techniques. J Pharmacokinet Biopharm 1988; 16:303 – 9.

33. Yuan J. Estimation of variance for AUC in animal studies. J Pharm Sci 1993;82:761 – 3.

34. Tukey RH, Strassburg CP. Human UDP-glucuronosyltransferases: metabolism, expression, and disease. Annu Rev Pharmacol Toxicol 2000; 40:581 – 616.

35. Tegner K, Nilsson HT, Persson CG, Persson K, Ryrfeldt A. Elimination pathways of terbutaline. Eur J Respir Dis Suppl 1984;134:93 – 100.

36. Davies B, Morris T. Physiological parameters in laboratory animals and humans. Pharm Res 1993;10:1093 – 5.

37. Berman J, Halm K, Adkison K, Shaffer J. Simultaneous pharmacokinetic screening of a mixture of compounds in the dog using API LC/MS/MS analysis for increased throughput. J Med Chem 1997;40:827 – 9.

38. Allen MC, Shah TS, Day WW. Rapid determination of oral pharmacokinetics and plasma free fraction using cocktail approaches: methods and application. Pharm Res 1998;15:93 – 7.

39. Macdonald SJ, Dowle MD, Harrison LA, et al. Discovery of further pyrrolidine *trans*-lactams as inhibitors of human neutrophil elastase (HNE) with potential as development candidates and the crystal structure of HNE complexed with an inhibitor (GW475151). J Med Chem 2002;45: 3878 – 90.

40. Borga O, Lindberg C. Pharmacokinetic implications of slow equilibration of terbutaline between plasma and erythrocytes. Eur J Respir Dis Suppl 1984;134:73 – 80.

41. Gromov PS, Celis JE. Identification of two molecular chaperons (HSX70, HSC70) in mature human erythrocytes. Exp Cell Res 1991;195: 556 – 9.

Molecular Cancer Therapeutics

Preclinical pharmacokinetics and metabolism of a novel diaryl pyrazole resorcinol series of heat shock protein 90 inhibitors

Nicola F. Smith, Angela Hayes, Karen James, et al.

Mol Cancer Ther 2006;5:1628-1637.